IJMMM International Journal of Minerals, Metallurgy and Materials 矿物冶金与材料学报（英文版）

Titanium microalloying of steel: A review of its effects on processing, microstructure and mechanical properties

Shuize Wang, Zhijun Gao, Guilin Wu, and Xinping Mao

Cite this article as:
Shuize Wang, Zhijun Gao, Guilin Wu, and Xinping Mao, Titanium microalloying of steel: A review of its effects on processing, microstructure and mechanical properties, *Int. J. Miner. Metall. Mater.*, 29(2022), No. 4, pp. 645-661. https://doi.org/10.1007/s12613-021-2399-7

International Journal of Minerals, Metallurgy and Materials
Volume 29, Number 4, April 2022, Page 645
https://doi.org/10.1007/s12613-021-2399-7

Invited Review

Titanium microalloying of steel: A review of its effects on processing, microstructure and mechanical properties

Shuize Wang[1,2),*], *Zhijun Gao*[1),*], *Guilin Wu*[1,2)], *and Xinping Mao*[1,2),✉]

1) Beijing Advanced Innovation Center for Materials Genome Engineering, University of Science and Technology Beijing, Beijing 100083, China
2) Guangdong Laboratory for Materials Science and Technology, Yangjiang Branch (Yangjiang Advanced Alloys Laboratory), Yangjiang 529500, China
(Received: 12 October 2021; revised: 16 December 2021; accepted: 20 December 2021)

Abstract: Carbon neutrality of the steel industry requires the development of high-strength steel. The mechanical properties of low-alloy steel can be considerably improved at a low cost by adding a small amount of titanium (Ti) element, namely Ti microalloying, whose performance is related to Ti-contained second phase particles including inclusions and precipitates. By proper controlling the precipitation behaviors of these particles during different stages of steel manufacture, fine-grained microstructure and strong precipitation strengthening effects can be obtained in low-alloy steel. Thus, Ti microalloying can be widely applied to produce high strength steel, which can replace low strength steels heavily used in various areas currently. This article reviews the characteristics of the chemical and physical metallurgies of Ti microalloying and the effects of Ti microalloying on the phase formation, microstructural evolution, precipitation behavior of low-carbon steel during the steel making process, especially the thin slab casting and continuous rolling process and the mechanical properties of final steel products. Future development of Ti microalloying is also proposed to further promote the application of Ti microalloying technology in steel to meet the requirement of low-carbon economy.

Keywords: titanium microalloying; precipitation; grain refinement; phase transformation; high-strength steel

1. Introduction

Currently, the steel industry requires green growth and carbon dioxide emission reduction to achieve carbon neutrality [1–2]. Increasing the strength of steel can indirectly reduce energy consumption and carbon dioxide emissions during the use of steel, which is an important development direction for the future of the steel industry [3]. The addition of a small amount of strong carbide-forming or nitride-forming elements, such as titanium (Ti), niobium (Nb), vanadium (V), and molybdenum (Mo), with contents generally no more than 0.1wt% to 0.2wt% in low-alloyed steel or manganese steel can significantly increase the strength of steels [4–5]. This technology is called the microalloying of steel. By applying the microalloying technique, the grain size of steel can be effectively refined and a large number of nano-sized precipitates can be developed at defects such as grain boundaries and dislocations, which can significantly increase the strength without sacrificing the plasticity and toughness of steel [6–12].

Ti, one of the most important microalloying elements, exists in steel in the form of solid solution and precipitation. Ti significantly affects the strength and toughness of steel either through solute drag or through the dissolution and precipitation behavior of secondary phases [13–14]. Moreover, Ti plays a significant role in improving the hardenability of steel and fixing nonmetallic elements. As an effective approach to improve the properties and performance of steel, Ti microalloying technology has been widely applied in steels used in fields, such as automobiles, construction, and machinery [15–16].

Grain refinement can increase the strength of materials according to the Hall–Petch equation, which quantifies the relationship between grain size and strength [17–18]. In the 1960s, Morrison [19] showed that precipitation strengthening and grain refinement can be obtained through the formation of precipitation in high-strength low-alloy steel. Subsequently, Davenport *et al.* [20] discovered nano-sized precipitates in the matrix of low-alloy steel. These particles can hinder the movement of dislocations, resulting in a strong strengthening effect. Thus, grain refinement strengthening and precipitation strengthening, which are the theoretical bases for the development of microalloyed steel, have been established and utilized as typical approaches to improve the strength of low-alloy steel.

In the 1970s, the conference "Microalloying 75" summarized the studies on microalloying of steel and proposed the idea of producing a new generation of high-strength steel through microalloying [21]. Subsequently, thermomechanical controlled processing (TMCP) was employed and considerably improved the mechanical properties of microalloyed

*These authors contributed equally to this work.
✉ Corresponding author: Xinping Mao E-mail: xinpingmao@ustb.edu.cn

steel.

In the 1990s, the conference "Microalloying 95" summarized the studies on microalloying of steel for the past 20 years and proposed two types of controlled rolling technology, i.e., recrystallization-controlled rolling (RCR) and non-recrystallization-controlled rolling (CCR), for the production of high-performance steel. Meanwhile, the concept of new-generation TMCP technology was also proposed [22]. The development of TMCP for microalloyed steel further promoted the development of microalloying theory and technology, which has attracted considerable attention worldwide.

Despite extensive studies, Ti microalloying technology has not been widely used in the steel industry for a long time. One reason is the high chemical activity of Ti. Ti easily combines with O, N, and S during metallurgy, resulting in the formation of large-sized inclusions. Thus, the amount of effective Ti is reduced [23]. Consequently, the precipitation behavior of Ti is changed, significantly decreasing the strength and stability of steel. Moreover, the formation of TiC is sensitive to temperature and cooling rate. Any fluctuation in the parameters of the production process has a direct effect on TiC precipitates, leading to large fluctuations in the mechanical properties of different steel plates or different parts of the same plate. Therefore, Ti microalloying technology has high requirements for controlling both chemical and physical metallurgies [24].

Since the 1990s, remarkable developments in Ti microalloying technology have been made with the progress of clean steel smelting technology and thin slab casting and direct rolling (TSCR) process. Ti microalloying technology-based TSCR has been finally developed [25–26]. Extensive studies on the microstructure, precipitation behavior, strengthening mechanism, and process control of Ti-microalloyed high-strength steel have been conducted [27–31]. Meanwhile, large-scale industrial production was also implemented.

With the development of Ti microalloying technology, a series of Ti-microalloyed steels with different strength grades were developed and used in civil engineering and other areas. At present, the widely used low-strength steel needs to be replaced with low-cost and high-strength steel in the context of a low-carbon economy. Ti microalloying will become one of the directions for microalloyed steel and high-strength steel because of its cost advantage and exceptional potential for strengthening and toughening. This article reviews the precipitation, recrystallization, and phase transformation of Ti-microalloyed steel and Ti-based multiple microalloying technology for Ti-microalloyed steel in recent years.

2. Physical properties of Ti and Ti compounds

Ti is a transition element with an atomic number of 22 and is located in the IV subgroup of the fourth period in the periodic table. Ti is a strong carbonitride-forming and nitride-forming element that can form stable compounds with non-metallic elements, such as O, N, and C. Ti is abundant in the earth's crust, with an abundance of approximately 0.63%.

Ti was first discovered by R.W. Gregor in ilmenite and rutile in 1791. American chemist Hunter obtained Ti with a purity of 99.9% for the first time in 1910 [32]. Kroll further developed a method to produce Ti in large quantities in 1938 [33–34].

Ti is usually added to steel as a microalloying element and exists in the form of titanium nitride (TiN), TiS, TiC, and $Ti_4C_2S_2$. Both TiN and TiC are interstitial phases with a NaCl-type (B1) face-centered cubic structure, and their lattice constants are a = 0.4239 nm and a = 0.43176 nm, respectively. The ratio of C and N atomic radii to Ti atomic radius is less than 0.59, leading to the completely miscible form of TiC_xN_{1-x} ($0 \le x \le 1$). TiS is a NiAs-type hexagonal crystal structure with lattice constants of a = 0.341 nm and c = 0.570 nm. $Ti_4C_2S_2$ also has a hexagonal crystal structure with lattice constants of a = 0.3209 nm and c = 1.1210 nm. The schematic diagram of the crystal structures of TiN, TiS, and $Ti_4C_2S_2$ is shown in Fig. 1.

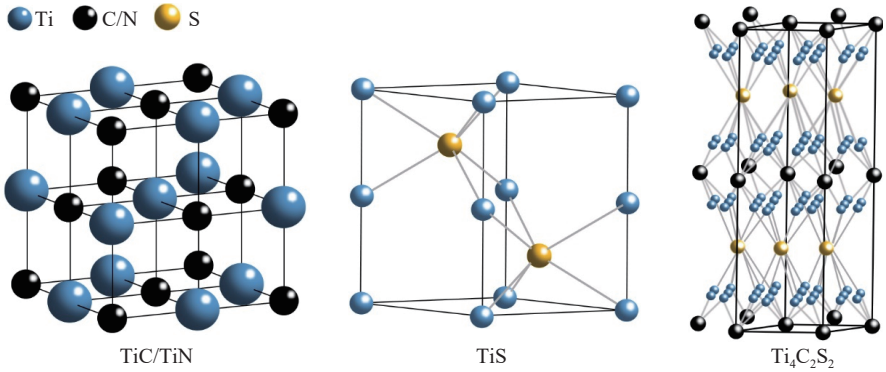

Fig. 1. Crystal structures of TiC, TiN, TiS, and $Ti_4C_2S_2$ [35].

China has the largest reserves of Ti resources, which account for 45.6% of the world's total reserves. Although microalloying elements, such as Nb, V, and Ti, are widely used in the steel industry, the cost of Ti microalloying is only one-fifth to one-seventh of those of Nb and V with the same strengthening effect. Ti microalloying technology has the most significant effects on microstructure refinement and comprehensive performance improvement. The application and popularization of Ti microalloying technology can provide infinite possibilities for the efficient and high-quality

utilization of Ti in steel. Therefore, the use of Ti resources and the development of Ti microalloying technology have considerable economic benefits and strategic significance for China.

3. Precipitation behavior in Ti-microalloyed steel

Precipitation of Ti-containing secondary phases is the most important issue in Ti microalloying technology. According to Orowan's theory [36], the strengthening effect of precipitation is directly proportional to the volume fraction and inversely proportional to the size of precipitates. By controlling the precipitation behavior, grain growth, recrystallization, and phase transformation can be effectively tailored during the microalloying process of steel. Thus, grain refinement can be enhanced and precipitation strengthening can be obtained, thereby considerably improving the strength of Ti-microalloyed steel. The key issues in theoretical studies and manufacturing practices of Ti-microalloyed steel include: (i) controlling the precipitation behavior of secondary phases, (ii) accurately tailoring the amount, shape, size, and distribution of precipitated particles, and (iii) improving the microstructure and performance of Ti-microalloyed steel.

As a strong carbonitride-forming element, Ti has a maximum solubility of 0.69% in austenite, a solubility of 1.24% at the phase boundary between austenite and ferrite, and a maximum solubility of 8.4% in ferrite. Moreover, the solubility of Ti in ferrite is significantly affected by temperature, e.g., the solubility at 873 and 673 K is 0.53% and 0.15%, respectively. Therefore, as the temperature decreases, Ti can form a large number of precipitates with different sizes and morphologies in the prior austenite grains and the final supersaturated ferrite during phase transformation.

Fig. 2 shows the precipitation procedure of Ti-bearing secondary phase particles developing at different stages during the TSCR process. Ti_2O_3 and TiN particles with relatively large sizes (in micron scale) are precipitated from molten steel during the smelting process, which plays a role in controlling the as-cast microstructure [37–38]. Fine TiN and $Ti_4S_2C_2$ particles with sizes ranging from tens of nanometers to hundreds of nanometers are precipitated in the solid state during the cooling process of the cast slab, which can control the grain size of austenite during soaking and hot rolling. TiC particles with sizes ranging from a few nanometers to tens of nanometers are formed through deformation induced by precipitation during hot rolling, which can postpone the recovery and recrystallization of austenite. TiC particles with sizes less than 10 nm are formed through interphase precipitation and supersaturation precipitation during the final rapid cooling and coiling, which can produce significant precipitation strengthening effect [34].

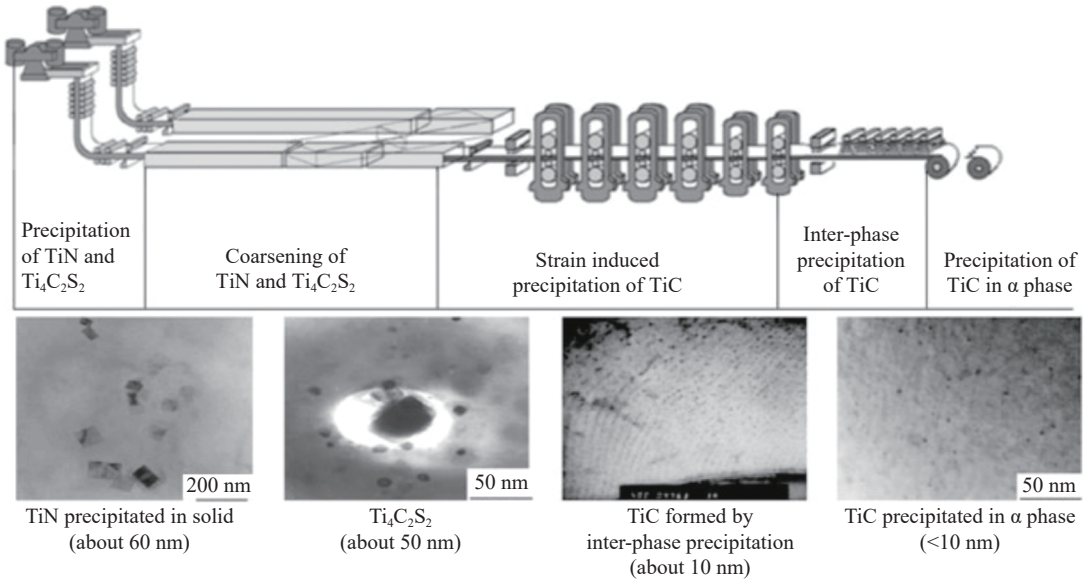

Fig. 2. Titanium-bearing precipitation in different stages during the thin slab casting and direct rolling process [35].

3.1. Titanium oxide

At high temperatures, Ti has a strong affinity with O, as expressed in Eq. (1), and titanium oxides are easily precipitated during the steelmaking process.

$$\lg([Ti]_\gamma[O]_\gamma) = 2.03 - 14440/T \text{ [39]} \quad (1)$$

where T is temperature; $[Ti]_\gamma$ and $[O]_\gamma$ are the corresponding element contents in austenite. Consequently, Fe–Ti alloy is usually added after deoxidation using Al–Si alloy or full deoxidation using Al. Thus, effective Ti needs to be used to generate a part of small Ti-containing oxides. However, over-oxidation of Ti should be also avoided to achieve a high yielding rate for Ti.

Titanium oxide has high stability at high temperatures and can pin austenite grain boundaries during the hot rolling process. By properly controlling the size and quantity of titanium oxides, the grain size of austenite can be effectively refined. Meanwhile, the nucleation of intragranular ferrite (acicular/granular ferrite) on austenite grain boundaries can also be promoted, thereby resulting in improved weldability

and toughness of steel [40].

According to the phenomenon of inclusions-induced intragranular acicular ferrite in different compositions, steel grades, and process conditions, four different mechanisms have been proposed [41–44]. (i) Solute-element-poor zone mechanism: Mn-poor regions in the matrix around Ti_2O_3 and C-poor regions around $Fe_{23}(C,B)_6$ or $Fe_3(C,B)$ increase the driving force for the transformation of austenite to ferrite. (ii) Cation vacancy mechanism: Titanium oxides, such as Ti_2O_3, are rich in cation vacancies, which provide channels for the diffusion of Fe and other metallic atoms, and become nucleation points for MnS and TiN to form composite inclusions, thereby promoting intragranular ferrite nucleation. (iii) Strain induction mechanism: Because of different linear expansion coefficients between inclusions and austenite, the interfaces between these two phases are distorted during the cooling process, providing activation energy for ferrite nucleation. (iv) Low mismatch mechanism: Nonmetallic inclusions with a structure similar to ferrite crystal structure can reduce the interfacial energy of ferrite nucleation; thus, the low-energy interfaces have low interface energy and stress–energy barrier.

Based on these four mechanisms, a series of Ti-related technologies, such as Ti treatment, Ti–Mg composite deoxidation, Ti–Al composite deoxidation, and Al–Ti–Mg composite deoxidation, have been developed to control the disperse nonmetallic inclusions and the microstructure of Ti-microalloyed steel. These techniques can refine the grain size of austenite, promote the formation of intragranular acicular ferrite, and improve the strength and toughness of steel.

3.2. Titanium nitride

TiN is chemically stable. The melting point of TiN is as high as 3203 K. Because the heat of mixing between Ti and N is as low as −109 kJ/mol [45], the solubility product of TiN in liquid iron is relatively small, which ensures that TiN particles are easily precipitated in liquid iron. The solubility product of TiN in liquid iron can be expressed as follows:

$$\lg([\mathrm{Ti}]_L[\mathrm{N}]_L) = 4.46 - 13500/T \text{ [46]} \quad (2)$$

$$\lg([\mathrm{Ti}]_L[\mathrm{N}]_L) = 5.922 - 16066/T \text{ [38]} \quad (3)$$

$$\lg([\mathrm{Ti}]_L[\mathrm{N}]_L) = 5.90 - 16586/T \text{ [47]} \quad (4)$$

where $[Ti]_L$ and $[N]_L$ are the amounts of Ti and N dissolved in liquid iron in wt%, respectively. Fig. 3 shows a linear relationship between the solubility products of TiN and the temperature in liquid iron.

For face-centered cubic crystals, {100} and {111} planes have the smallest surface energies. Thus, TiN usually presents in a cubic or polygonal shape, as shown in Fig. 4.

TiN precipitates formed during the solidification process are often small, usually in the size of ~100 nm. TiN precipitates can effectively suppress the growth of austenite grains during heating or isothermal solid solution treatment. Highly dispersed TiN particles in submicron scale could efficiently pin the austenite grain boundaries, and their pinning effect can be kept up to 1573 K [48]. Meanwhile, they can also act as heterogeneous nucleation sites for ferrite, promoting grain

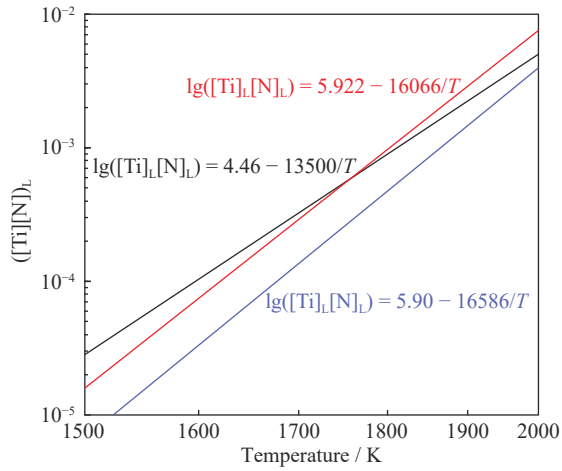

Fig. 3. Solubility products of TiN in liquid iron [35].

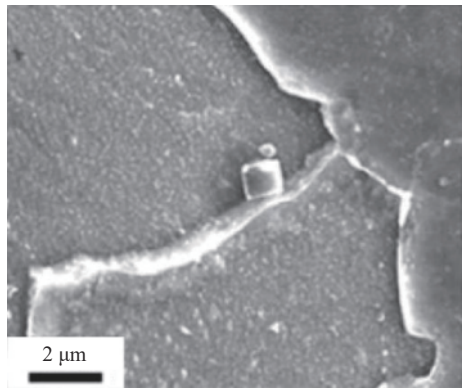

Fig. 4. Cubic TiN formed in liquid iron [35].

refinement and the formation of equiaxed grains, thereby enhancing the mechanical properties of steel. Kuziak *et al.* [49] investigated the refining effect of N and microalloying elements on the solidification structure of ferrite–pearlite steel. They determined that TiN had an effective refining effect even when the Ti content was less than 0.01wt%, provided that the N content reached 150–200 ppm. Lee *et al.* [50] analyzed the effect of Ti addition on nonmetallic inclusions and solidification structure in low-carbon forged steel. They determined that an increase in Ti content from 48 to 120 ppm promoted the formation of TiN particles and reduced the original grain size of austenite.

TiN particles formed in liquid iron are generally larger than 0.5 μm. Because of their coarse particle size and low number density, TiN particles cannot effectively prevent grain growth and has a small strengthening effect. Xing *et al.* [51] measured the size of TiN after solidification. As shown in Fig. 5, sharp edges and corners are observed in TiN precipitates. The maximum size even reaches 5 μm, which negatively affects the performance of steel.

Micron-sized TiN formed in liquid iron could weaken the interface between TiN and matrix. These interfaces could become crack sources or crack propagation channels during plastic deformation (see Fig. 6) [52], significantly deteriorating the toughness of steel. Moreover, these micron-sized TiN particles can neither pin the austenite grain boundaries nor achieve strong precipitation strengthening effect. They also

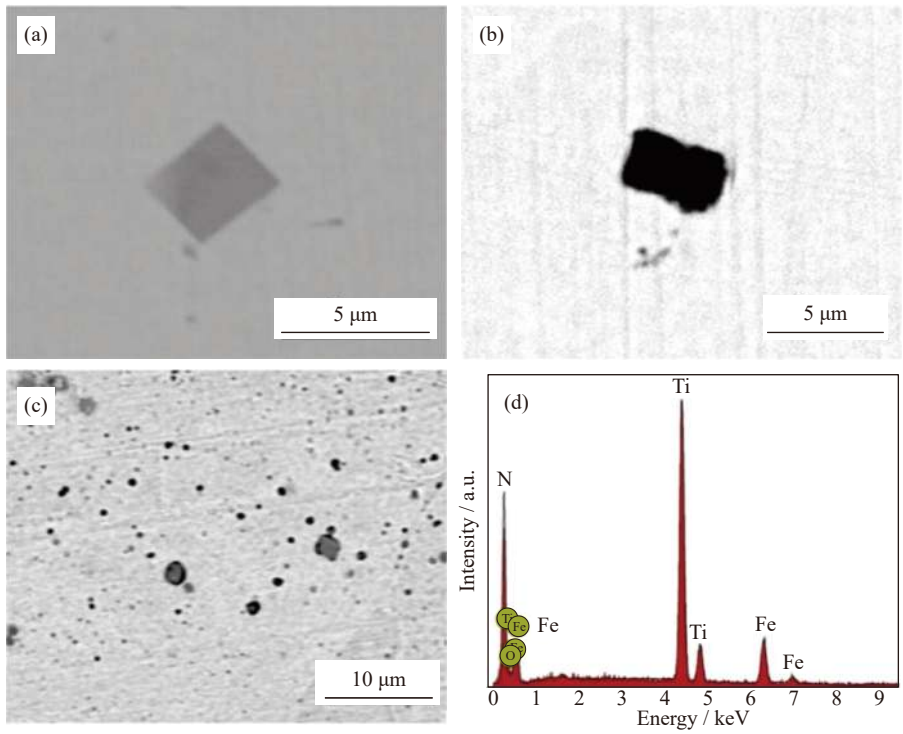

Fig. 5. (a–c) Different TiN precipitates and (d) the energy dispersive spectroscopy of precipitates. Adapted from *Mater. Today Commun.*, 25, L.D. Xing, J.L. Guo, X. Li, Z.F. Zhang, M. Wang, Y.P. Bao, F.Z. Zeng, and B.T. Chen, Control of TiN precipitation behavior in titanium-containing micro-alloyed steel, 101292, Copyright 2020, with permission from Elsevier.

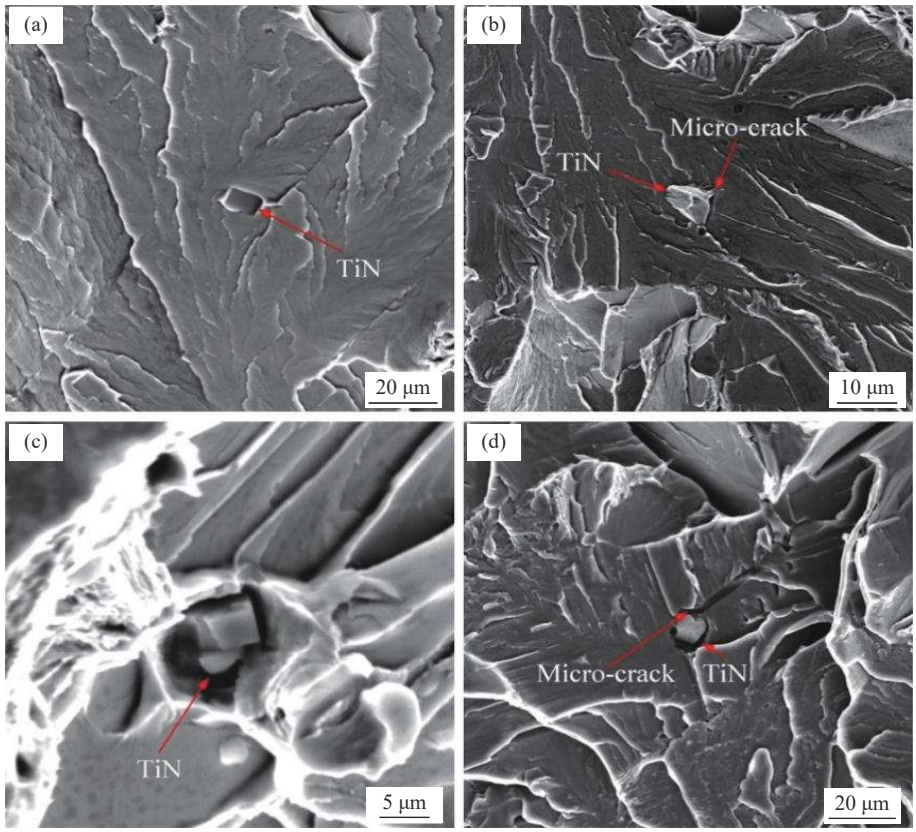

Fig. 6. Microcrack initiated from TiN particles. Reprinted by permission from Springer Nature: *J. Iron Steel Res. Int.*, Effect of coarse TiN inclusions and microstructure on impact toughness fluctuation in Ti micro-alloyed steel, T. Liu, M.J. Long, D.F. Chen, H.M. Duan, L.T. Gui, S. Yu, J.S. Cao, H.B. Chen, and H.L. Fan, Copyright 2018.

consume the effective Ti in steel. Fu *et al.* [53] reported that the size of TiN formed in liquid iron was in the range of 1–3 μm in steel containing 0.025wt% to 0.045wt% Ti and 0.045wt% to 0.07wt% N. Yang *et al.* [54] further confirmed

that the size of TiN formed in liquid iron was related to the contents of Ti and N and the cooling rate. They showed that low contents of Ti and N and high cooling rate both facilitate the formation of fine TiN particles in liquid iron. The ideal stoichiometric ratio of Ti/N in steel is 3.42. When the stoichiometric ratio is higher than 3.42, coarse TiN particles will be formed.

3.3. Titanium sulfide

In addition to the presence of TiN precipitates at high temperatures, Ti may also precipitate in the form of sulfides or sulfur carbides in high-temperature austenite of steel. The related solid solubility product formulas are expressed as follows:

$$\lg([\mathrm{Ti}]_\gamma[\mathrm{N}]_\gamma) = 4.22 - 14200/T \text{ [55]} \quad (5)$$

$$\lg([\mathrm{Ti}]_\gamma[\mathrm{S}]_\gamma) = 5.43 - 13975/T \text{ [56]} \quad (6)$$

$$\lg([\mathrm{Ti}]_\gamma[\mathrm{C}]_\gamma^{0.5}[\mathrm{S}]_\gamma^{0.5}) = 6.32 - 15350/T \text{ [57]} \quad (7)$$

$$\lg([\mathrm{Ti}]_\gamma[\mathrm{C}]_\gamma) = 3.21 - 7480/T \text{ [55]} \quad (8)$$

where $[\mathrm{Ti}]_\gamma$, $[\mathrm{N}]_\gamma$, $[\mathrm{S}]_\gamma$ and $[\mathrm{C}]_\gamma$ are the amounts of Ti, N, S and C in austenite in wt%, respectively. Fig. 7 shows the solid solubility products of TiO, TiN, TiS, $Ti_4S_2C_2$, and TiC in austenite. The precipitation order is usually in the sequence of TiN→TiS→$Ti_4S_2C_2$ from high to low temperatures. Notably, at temperatures above 1523 to 1573 K, TiS will precipitate before $Ti_4S_2C_2$. Meanwhile, below this temperature range, $Ti_4S_2C_2$ precipitation will dominate.

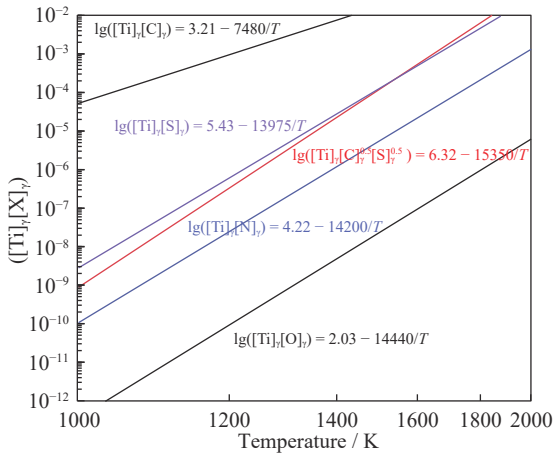

Fig. 7. Solid solubility products of Ti-bearing secondary phases in austenite [35]. X represents the corresponding nonmetallic element C, N, or S.

The size ranges of TiS and $Ti_4S_2C_2$ precipitates are relatively large. Small ones are only tens of nanometers, and large ones can reach several micrometers. These two precipitates have both spherical and hexagonal morphologies. Yu *et al.* [58] investigated the precipitation behavior of TiS and $Ti_4S_2C_2$ in Fe–0.002C–0.16Mn–0.0016N–0.0028S–0.07Ti (wt%) steel during the TSCR process. Long rod-like and irregular-shaped TiS precipitates with the size of approximately hundreds of nanometers were detected. The typical morphology of TiS precipitates is shown in Fig. 8. Jing *et al.* [59] observed spherical or worm-like TiS and $Ti_4S_2C_2$ precipitates with the size of approximately 3–6 μm in their experimental steel, which was produced through hot rolling and air cooling combined with subsequent tempering at 1023 K for 3 h.

When analyzing Fig. 7, the influence of the contents of Ti, Mn, S, and other related elements in steel must be considered. For example, the precipitation of TiS will be significantly inhibited in IF steel because C has a significantly higher content than S. Thus, the precipitation order is changed to TiN→$Ti_4S_2C_2$→TiC.

Liu *et al.* [60] estimated the Gibbs free energy for the formation of TiS and $Ti_4S_2C_2$ in austenite and determined that $Ti_4S_2C_2$ was preferentially precipitated in steel with a high Ti content. TiS and $Ti_4S_2C_2$ might exist at the same time in micro-Ti treated steel with a low Ti content. Yoshinaga *et al.* [61] reported that, when heated at 1373 K, the fraction of $Ti_4S_2C_2$ tended to decrease and the fraction of TiS tended to increase as the S content increased with a fixed Ti content (0.02wt%). However, the fraction of $Ti_4S_2C_2$ tended to increase and the fraction of TiS tended to decrease as the Ti content increased with a fixed S content (0.02wt%). Yan and Zhang [62] observed that strip-shaped MnS formed in micro-Ti treated steel with a high S content (0.026wt%). However, the fraction of MnS tended to decrease and the fraction of $Ti_4S_2C_2$ tended to increase with the increase in Ti content. When the Ti content reached 0.11wt%, elongated MnS was nearly completely replaced by dispersed spherical $Ti_4S_2C_2$.

Among all sulfides, strip-shaped MnS can be easily changed to elongated inclusions during the rolling process, forming a band-like structure, which aggravates the difference in toughness and ductility of rolled steel between rolling and transverse directions. The reaction of Ti and S can form hard-to-deformed $Ti_4S_2C_2$ particles in steel, which prevents the reaction of Mn and S to MnS, normally extending into band-like inclusions along the rolling direction. Therefore, the addition of Ti can optimize the morphology and distribution of sulfides, which can reduce the hot brittleness caused by MnS, improve the cold forming performance, and mitigate the performance anisotropy by reducing the difference between vertical and horizontal properties of steel plates.

With the same Ti addition, the fluctuation of O, S, and N contents directly affects the precipitation behavior of TiC, leading to the fluctuation of the mechanical properties of the final steel product. Therefore, the mass fractions of O, S, and N should be reduced and stabilized during steel manufacturing to increase the microstructure stability and hence the product quality. The contents of O, S, and N should be controlled in the ranges of <0.0025wt%, <0.005wt%, and <0.007wt%, respectively. Smelting such clean molten steel is possible with the development of modern metallurgical technologies.

3.4. Interphase precipitation

According to the different nucleation sites, precipitation can be divided into interphase precipitation and dispersion precipitation. When carbides, nitrides, and carbonitrides repeatedly nucleate at the γ/α interfaces and pass through austenite grains, band precipitation occurs during the transform-

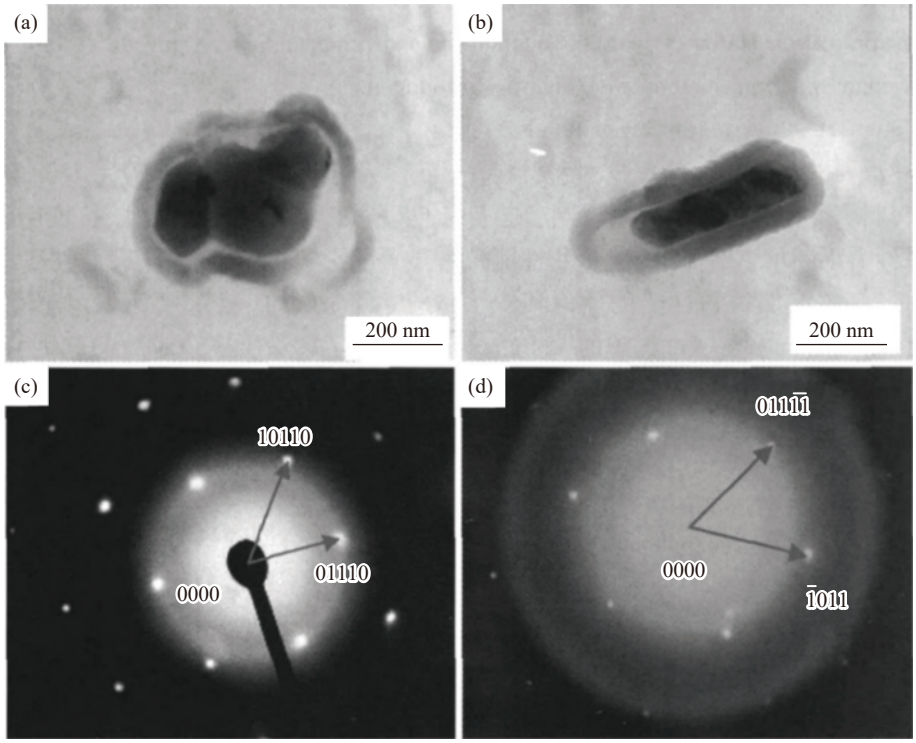

Fig. 8. (a, b) Transmission electron microscope morphologies and (c, d) diffraction patterns of the TiS particles [58].

ation from austenite to ferrite, which is called interphase precipitation. The special precipitation form in steel was detected for the first time in 1964, in which NbC, V(C,N), TiC, and (Ti,Mo)C can all precipitate during the phase transition [63–64]. Precipitation between phases can be divided into discrete precipitation and fibrous precipitation based on particle shapes (see Fig. 9) [65]. Generally, fibrous precipitates are larger and often appear in steel with high alloy contents. Meanwhile, discrete precipitates are mostly observed in Ti-microalloyed steel, mainly in the form of fine and dispersed TiC columns with a size between 5 nm and 15 nm, which have strong precipitation strengthening effect.

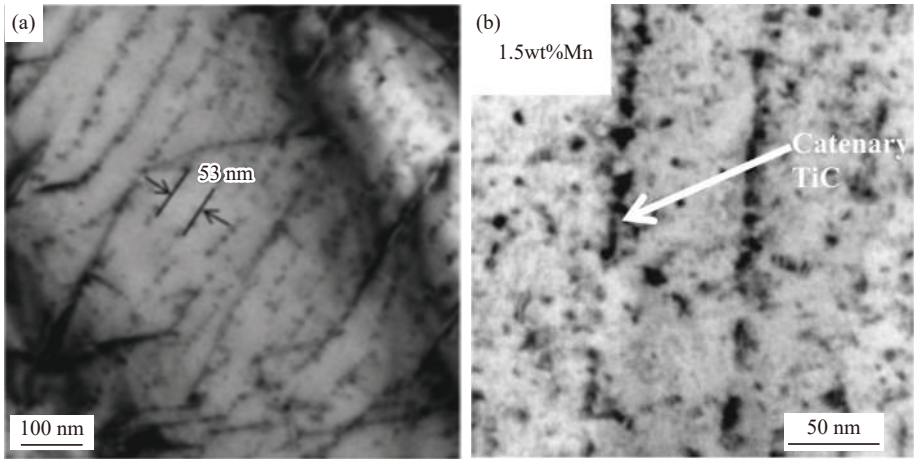

Fig. 9. (a) Discrete interface precipitations and (b) fibrous interface precipitations in microalloyed steel [35].

Interphase precipitation can be divided into planar interphase precipitation with the same interplanar spacing (PIP), curved interphase precipitation with irregular interplanar spacing (irregular-CIP), and curved interphase precipitation with the same interplanar spacing (regular-CIP) (see Fig. 10) [66–67].

PIP is formed through a step mechanism at the partially continuous γ/α interfaces (see Fig. 10(a)). Precipitation nucleates and grows on the interfaces and moves to the next step. When carbonitrides are formed on semi-coherent phase boundary planes, the phase boundaries have low energy and are immovable. Thus, phase transformation is mainly initiated by high-energy ferrite step movement. When austenite transforms into ferrite, the Kurdjumov–Sachs (K-S) orientation relationship, i.e., $\{110\}_{\alpha}\|\{111\}_{\gamma}$, would keep between the two phases. Meanwhile, the interphase precipitation in Ti-microalloyed steel and ferrite matrix form a Baker–Nutting (B-N) orientation relationship, i.e., $\{100\}_{CN}\|\{100\}_{\alpha}$ and $\{110\}_{CN}\|\{111\}_{\alpha}$. Therefore, interphase precipitation lies along 45° or 90° to the γ/α interfaces. However, Yen

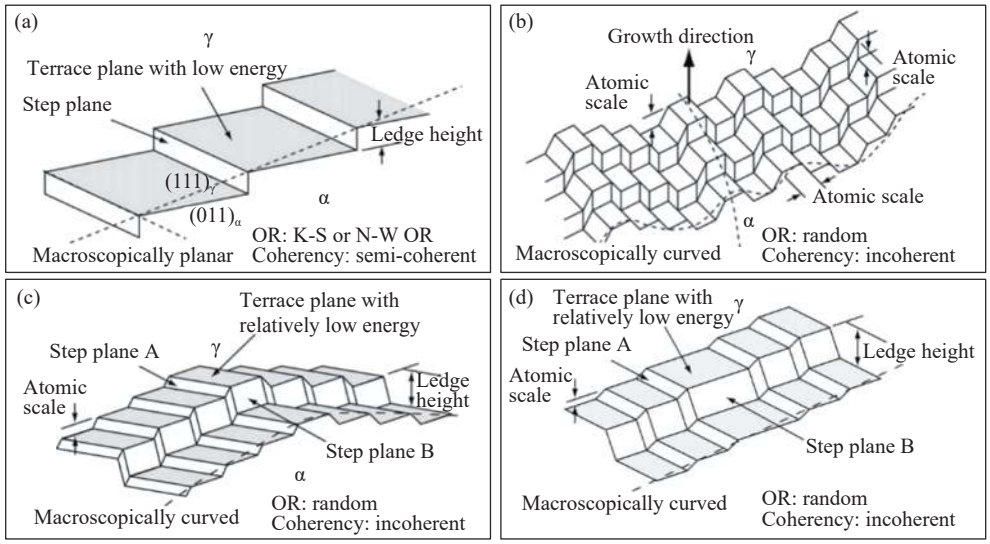

Fig. 10. Schematic diagram of the interphase precipitation formation mechanism: (a) planar interphase precipitation with the same interplanar spacing, (b) curved interphase precipitation with irregular interplanar spacing, (c) curved interphase precipitation with the same interplanar spacing, and (d) PIP at the incoherent γ/α interfaces. OR represents orientation relationship. Reprinted from *Acta Mater*., 59, H.W. Yen, P.Y. Chen, C.Y. Huang, and J.R. Yang, Interphase precipitation of nanometer-sized carbides in a titanium–molybdenum-bearing low-carbon steel, 6264-6274, Copyright 2011, with permission from Elsevier.

et al. [67] discovered that the relationship between TiC phase precipitation and ferrite matrix in Ti-microalloyed steel (0.185Ti) changed from the B-N orientation relationship to the Nishiyama–Wassermann (N-W) orientation relationship, i.e., $(111)_{TiC}\|(011)_{\alpha}$, $[1\bar{1}0]_{TiC}\|[111]_{\alpha}$ and $(\bar{1}\bar{1}\bar{1})_{TiC}\|(0\bar{1}1)_{\alpha}$, $[1\bar{1}0]_{TiC}\|[100]_{\alpha}$, during the progress of isothermal transformation.

Irregular-CIP is related to the movement of incoherent γ/α phase interfaces (see Fig. 10(b)). The microalloying element Ti can segregate at the phase interfaces and inhibit the movement of interfaces so that the microalloy carbonitride has sufficient time to randomly nucleate at the interfaces. The γ/α phase interfaces can easily hinder the inhibition of precipitated particles through the arching mechanism, where particle spacing is large. Interfaces move forward until they are restrained again and their moving rates slow down to facilitate the nucleation of precipitates at the interfaces. This process is repeated continuously. Thus, curved interphase precipitation is formed.

Regular-CIP can also precipitate at incoherent γ/α interfaces and nucleate at the hindered incoherent two-phase interfaces through the quasi-step mechanism (see Fig. 10(c)). When a moving phase boundary is dragged by alloying solutes, the speed of the phase boundary slows down so that interphase precipitates nucleate on it, thereby effectively preventing the movement of the phase boundary. As the precipitated embryonic nucleus grows, the phase interface segment collapses along the direction perpendicular to the phase interface. Hence, ferrite continues to grow. Theoretically, there are three kinds of B-N orientation relationships. In practice, one kind of B-N orientation relationship is the result of energy minimization. The interphase precipitation along a specific direction can minimize the energy difference between the habitual plane and the phase interface [65]. Carbonitrides of microalloys nucleate at the high-energy γ/α phase interfaces. Thus, the movement of the phase boundary is inhibited by precipitation. Phase transformation is mainly initiated by high-energy ferrite steps along the direction perpendicular to the growth.

Discrete precipitation usually exhibits the same B-N orientation relationship [68]. In any given ferrite grain, this process is largely related to the mechanism of the α/γ interface propagating and translating through steps, which are difficult to grow because the steps themselves move too fast. The other researchers also observed the same interphase precipitation phenomenon in Ti-bearing and Nb-bearing [69–71] or V-bearing [72–73] microalloyed steel. In the investigated steels with different Ti contents, i.e., 0.55wt%, 0.25wt%, and 0.13wt%, austenite is directly transformed into ferrite through a subcritical isothermal transformation in the temperature range of 873 to 1073 K, and TiC appears in the form of thin ribbons during the γ→α transformation process. TiC precipitation has sizes of 2–5 nm, and their dispersion depends mainly on the temperature phase transformation.

Yen *et al.* [74] analyzed the crystallography and morphology of TiC particles in steel containing 0.10wt% C, 0.10wt% Si, 1.43wt% Mn, 0.185wt% Ti, and 41 ppm S. The steel was cast and rolled into 30 mm-thick plates, followed by austenitization at 1473 K, isothermal heat treatment at 1028 K for various times, and quenching. After a short annealing time, fine TiC flakes developed and kept a near B-N orientation relationship to the ferrite matrix. However, after a long annealing time, coarse TiC flakes had a near N-W orientation relationship to the ferrite matrix.

Yen *et al.* [67] and Okamoto *et al.* [75] analyzed the orientation relationship between PIP and ferrite matrix, as shown in Fig. 11. Honeycombe and Mehl [76] determined that the plane-type precipitation with regular interplanar spacing easily precipitated on the partially coherent $\{110\}_{\alpha}\|\{111\}_{\gamma}$ trapezoidal platform. Okamoto *et al.* [75] ob-

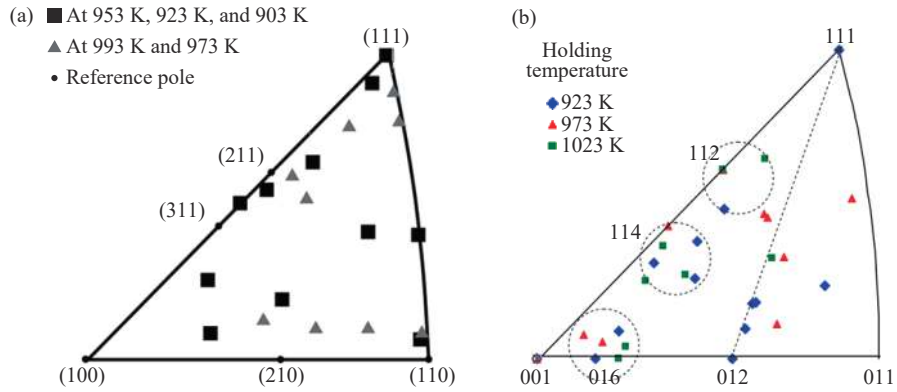

Fig. 11. Orientation distribution for interphase precipitation: (a) investigation of Yen *et al.*; (b) investigation of Okamoto *et al.* (a) Reprinted from *Acta Mater.*, 59, H.W. Yen, P.Y. Chen, C.Y. Huang, and J.R. Yang, Interphase precipitation of nanometer-sized carbides in a titanium–molybdenum-bearing low-carbon steel, 6264-6274, Copyright 2011, with permission from Elsevier; (b) Reprinted from *Acta Mater.*, 58, R. Okamoto, A. Borgenstam, and J. Ågren, Interphase precipitation in niobium-microalloyed steels, 4783-4790, Copyright 2010, with permission from Elsevier.

served that not all precipitates formed along $\{110\}_\alpha$ in Fe–Ti–Nb-microalloyed steel. With the progress of ferrite phase transformation, the formation of interphase precipitation can change from curved interphase precipitation to planar interphase precipitation, which shows that planar interphase precipitation can also form on the incoherent phase boundaries.

The morphology of interphase precipitation is mainly affected by the continuous cooling rate, isothermal temperature, and chemical composition [77–79]. The distance between the precipitation planes is closely related to the diffusion of the microalloying elements constituting the precipitated particles and the driving force of precipitation nucleation. The diffusion model of microalloying elements near the phase interface during isothermal transformation reveals that interplanar spacing is related to the concentration gradient of the precipitated phase elements near the interface. The width of the interplanar spacing, the size of the precipitated particles, and the square root of the diffusion rate of microalloying elements have a linear relationship [80–82]. The width of the interphase precipitation distance and the growth rate of the steps are related to the contents of microalloying elements in the interphase precipitated particles and the contents of interstitial elements near the steps along the phase interface. The interfacial distance depends on the diffusion distance of the microalloying elements in austenite. At the same time, the migration rate of the two-phase interface plays an important role in the generation and morphology of phase interface precipitation because it is accompanied by phase transition. The interphase precipitation surface spacing increases as the phase interface migration rate decreases.

3.5. Random precipitation

At temperatures lower than the interphase precipitation temperature, supersaturated ferrite precipitates randomly (see Fig. 12), particularly under deformation conditions [83]. The deformed matrix has high deformation energy, which can promote the recrystallization of austenite. Moreover, high-density dislocations and subgrain boundaries after deformation can provide a large number of nucleation sites for the precipitation of carbides. When the contents of Ti and C are relatively high, the temperature of TiC in a complete solution is higher than the solid solution temperature. Therefore, TiC can precipitate effectively in austenite, which can inhibit the recrystallization of austenite, resulting in a fine microstructure through controlled rolling.

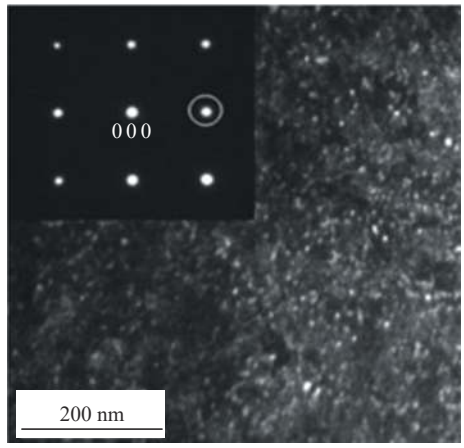

Fig. 12. Random precipitation in supersaturated ferrite [35].

In Ti-microalloyed steel, Ti usually precipitates in the form of TiC between 923 and 1023 K and mainly along dislocations. In ferrite, TiC precipitates have the size of a few nanometers and are uniformly distributed in ferrite, which exhibits a strong precipitation strengthening effect. In addition to rolling conditions, Mn, Mo, and other alloying elements also have significant effects on the precipitation of TiC. Notably, an increase in Mn content can significantly hinder the precipitation of TiC, and the pinning effect gradually decreases with the decrease in aging temperature (see Fig. 13) [84]. Thus, TiC precipitates in ferrite can be significantly refined through the co-addition of Mn and optimization of the rolling and coiling temperatures [84].

4. Recrystallization and phase transformation of Ti-microalloyed steel

Ti-microalloyed high-strength steel is mainly precipita-

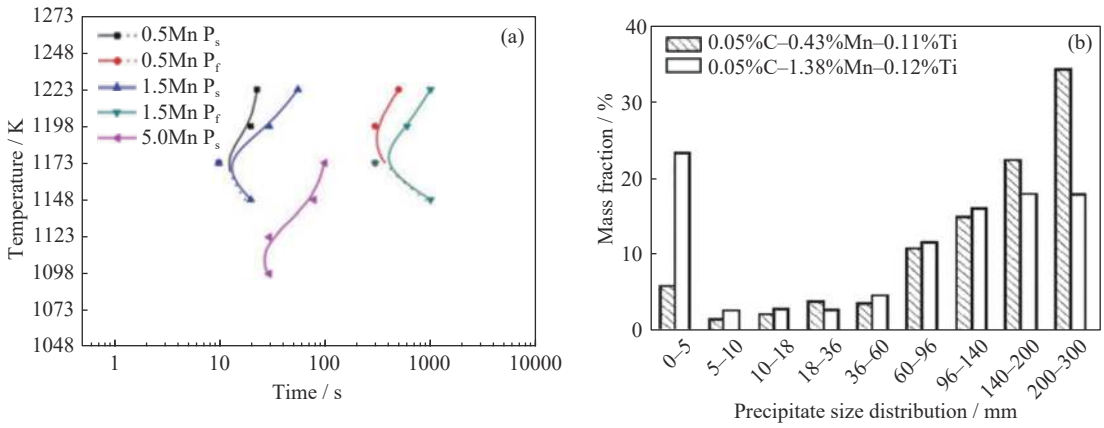

Fig. 13. Influence of different Mn contents on the precipitates in Ti-microalloyed steel: (a) precipitation-time–temperature diagram [35]; (b) precipitation size distribution with different Mn contents [84].

tion-strengthened ferritic steel. A good balance between ferrite grain refinement and TiC precipitation is important to ensure the high strength and toughness of steels. The refinement of ferrite grains depends both on the reduction of the grain size of austenite and on controlling the phase transition temperature. The refinement of austenite is mainly controlled by the grain growth of austenite during the austenitization stage and the dynamic recrystallization behavior during the hot rolling process. The actual phase transformation temperature of ferrite is controlled by the cooling process and alloying elements to reduce the phase transformation temperature as low as possible. The performance of cold-rolled Ti-microalloyed steel is also affected by the recrystallization behavior of cold-rolled ferrite.

4.1. Recrystallization behavior of austenite

One of the most significant features of microalloying elements is that they can affect the recrystallization of austenite during the CCR process. The two main methods are (i) to adopt controlled rolling to prevent the recrystallization of austenite deformed at high temperatures to achieve flat austenite grains, such that ferrite grains can be refined during phase transformation, and (ii) to apply controlled recrystallization rolling to recrystallize austenite grains repeatedly, such that austenite grains can be refined gradually. Different microalloying elements have different effects on the recrystallization of austenite. The higher the initial solute element contents are, the higher the termination temperatures of recrystallization. With the same atomic fraction, Nb has the best effect, followed by Ti and V. For the single Ti microalloying technique, the pinning force of TiN or Ti(C,N) is only half of the driving force of austenite recrystallization. Thus, RCR is usually applied. Medina *et al.* [85] investigated the effect of Ti content on the particle sizes of TiN and the grain sizes of austenite under different N contents and determined that micro-Ti treatment and single high-Ti microalloying can both effectively suppress the coarsening of austenite grains during the austenitization stage. When the mass ratio of Ti/N is 2–3, TiN has the best effect on suppressing the coarsening of austenite grains (see Fig. 14).

The research shows that different microalloying elements

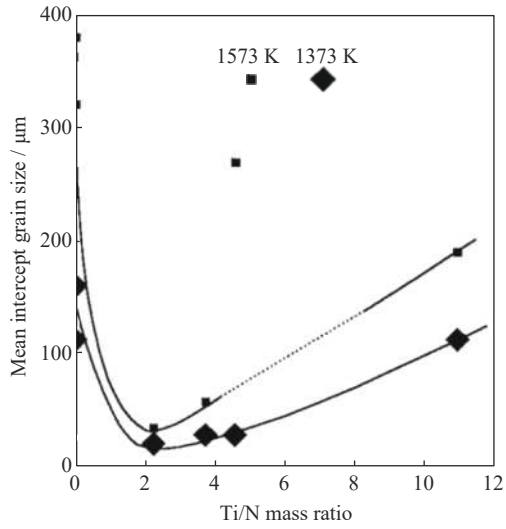

Fig. 14. Grain size of austenite against the mass ratio of Ti/N at 1373 K for 10 min and 1573 K for 10 min [85].

have a significant effect on austenite coarsening behavior [86]. If the temperature is higher than the temperatures for grain coarsening (TGC), the precipitates formed by microalloyed elements begin to dissolve and grow, and their pinning effect on austenite grains decreases so that austenite grains grow extensively. Therefore, TiN, Nb(C,N), and V(C,N) can suppress the coarsening of austenite grains at approximately 1523 K, 1423 K, and 1273 K, respectively. Notably, Ti has the highest critical temperature that can suppress the coarsening of austenite grains. Thus, Ti is considered the best element for microalloying. Moreover, 0.01wt% to 0.02wt% Ti is often added to steel to obtain good welding performance of steel so that excessive coarsening of austenite grains can be inhibited during the high-temperature welding process.

When deformed metals or alloys are annealed, recovery and recrystallization will occur. The driving force of recrystallization (F_{REX}) is expressed as follows:

$$F_{REX} = G\boldsymbol{b}^2\Delta\rho/2 \tag{9}$$

where G is the shear modulus of steel, $\boldsymbol{b}$ is the Bergs vector of dislocation, and $\Delta\rho$ is the difference in dislocation density of the matrix before and after recrystallization. Notably, the typ-

ical driving force for austenite recrystallization at low temperatures after single-pass rolling is approximately 20 MN/m^2 [87]. Such driving force for austenite recrystallization is approximately 200 times the driving force for austenite coarsening. This is an important basis for alloying design. If no other factors influence grain boundary migration during recrystallization, then the grain size of austenite after recrystallization is equivalent to the pre-austenite grain size. Precipitates of microalloys in steel nucleate preferentially at preexisting grain boundaries and deformation-introduced dislocations. These precipitates have a pinning effect on the migration of austenite grain boundaries during recrystallization. The pinning force (F_P) is expressed as follows [59]:

$$F_P = 6\sigma f I / \left(\pi d^2\right) \tag{10}$$

where σ is the grain boundary energy, f is precipitate volume fraction, I is the subgrain size, and d is precipitate average diameter. Notably, increasing the volume fraction of precipitates and reducing the average size of precipitates can effectively improve the pinning effect and prevent the recrystallization of the matrix. Fig. 15 shows the effect of microalloying elements on the termination temperature of recrystallization [88]. Nb has the best effect in preventing austenite recrystallization, whereas Ti has an intermediate effect and V and Al have the least effect. Moreover, deforming austenite at low temperatures promotes the precipitation of nano-sized TiC within austenite, thereby inhibiting the dynamic or static recrystallization of deformed austenite [34]. The addition of 0.1wt% Ti can significantly increase the static recrystallization temperature and extend the recrystallization time of deformed austenite. The addition of 0.20wt% Mo can further inhibit the recrystallization of TiC precipitation at 1198 K and below. Medina *et al.* [85] compared the static recrystallization and kinetics of deformation-induced precipitation of austenite in 0.042wt% Nb-, 0.095wt% V-, and 0.075wt% Ti-microalloyed steels. They determined that static recrystallization is more likely to occur in Ti-microalloyed steel compared with Nb- and V-microalloyed steels with similar contents of other elements.

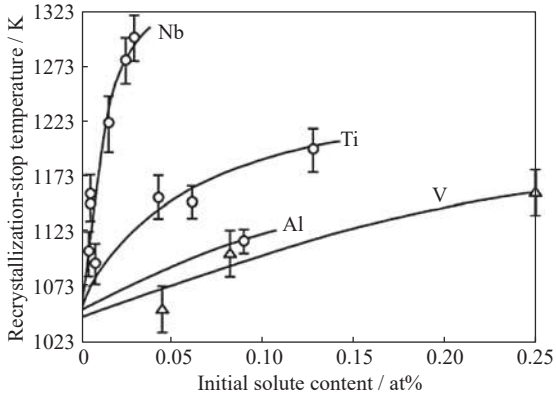

Fig. 15. Effect of the contents of the microalloying elements on the recrystallization of austenite during hot deformation [88]. Copyright 2003 from Niobium in modern steels by A.J. DeArdo. Reproduced by permission of Taylor and Francis Group, LLC, a division of Informapic.

4.2. Austenitic ferrite transformation behavior

The addition of microalloying elements in steel normally increases the chemical driving force of γ→α transformation and reduces the phase transformation temperature [89]. Thus, fine ferrite grain size can be obtained in the form of acicular ferrite or bainite. The microalloying elements also affect the volume fraction of bainite [90]. Nb has the best effect on the ferrite grain size and bainite volume fraction under accelerated cooling, Ti has the second best effect, and V has the least effect.

The transformation of supercooled austenite in Ti-microalloyed steel is a complicated process. The microstructures obtained after different cooling processes are quite different. The typical structures at room temperature are polygonal ferrite, quasi-polygonal ferrite, granular bainite, martensite, and retained austenite. These structures can be classified into five categories according to their shapes under the condition that undercooled austenite only undergoes ferrite transformation during the decomposition process, whereas retained austenite decomposes at a lower transformation temperature [91–93]. The main classifications are as follows:

(1) Polygonal ferrite: Polygonal ferrite mostly nucleates at the trigeminal grain boundary of deformed austenite and grows by diffusion [94]. Ferrite can exceed the original grain boundary of deformed austenite during growth. Polygonal ferrite is close to the equilibrium phase, and its chemical composition is quite different from that of deformed austenite. Therefore, the growth rate of polygonal ferrite is usually slow and is affected by the migration of replacement atoms and the long-range diffusion of C. The polygonal ferrite observed under optical microscopes is equiaxed with smooth grain boundaries.

(2) Widmanstatten ferrite: Widmanstatten ferrite is mostly formed in the continuous cooling phase transformation process, and its cooling rate and formation temperature are lower than those of polygonal ferrite [95]. The Widmanstatten ferrite grains are significantly elongated and coarser as observed under optical microscopes.

(3) Quasi-polygonal ferrite: Quasi-polygonal ferrite is formed by transformation at a lower transformation temperature [96], and it has the same chemical composition as deformed austenite. Atoms in the new phase do not need a long-range diffusion and only need to cross the phase boundaries. Thus, the transformation speed of quasi-polygonal ferrite is fast. Moreover, the diffusion and migration of atoms occur on the boundaries, leading to irregular growth and zigzag boundaries. Because of its high dislocation density, quasi-polygonal ferrite has high strength and good ductility.

(4) Granular ferrite: The formation temperature of granular ferrite is slightly lower than that of quasi-polygonal ferrite, which is a mid-temperature phase transformation product [42]. Granular ferrite is composed of elongated ferrite grain bundles. The matrix is distributed with a granular or equidistant structure. When forming at a slightly higher temperature, granular ferrite develops equiaxed subgrain and island-like structures with a disordered distribution in the mat-

rix. When forming at a slightly lower temperature, lath ferrite is formed and the distribution of island-like structures is more orderly. Ferrite grain bundles in granular form have a high dislocation density with a strong dislocation strengthening effect.

(5) Bainite ferrite: Bainite ferrite is also called lath ferrite and is composed of parallel ferrite lath bundles. The laths in bainite ferrite are parallel to each other, and the crystal orientation is nearly the same [97–98]. Therefore, lath bundles are high-angle boundaries, and lath boundaries are small-angle boundaries. Bainite ferrite grains have no clear characteristics observed under optical microscopes because it does not easily form erosion regions on small-angle boundaries. When there are retained austenite or M/A islands between ferrite grains, ferrite grains exhibit needle-like characteristics. Because lath bundles in bainite ferrite have small sizes and high-density dislocations, they exhibit high strength and high toughness.

4.3. Cold-rolled ferrite recrystallization behavior

Recrystallization annealing is a process in which a cold-deformed metal is heated to a temperature below A_1 (the temperature of ferrite to austenite transformation during heating) and above the recrystallization temperature, followed by cooling after holding for a certain period. Generally, the annealing process of cold-rolled Ti-microalloyed high-strength steel can be divided into three stages, i.e., recovery, recrystallization, and grain growth, and the effect of annealing temperature on complete recrystallization is more critical than that of annealing time.

The recrystallization temperature of cold-rolled Ti-microalloyed high-strength steel is as high as 988 K, which is significantly higher than that of ordinary cold-rolled low-carbon steel. Even when annealed at 903 K for a long time, no recrystallized grains with an equiaxed shape would appear in the microstructure.

Choi *et al.* [99] investigated the precipitation and recrystallization processes of two ultralow-carbon steels with distinct Ti contents. They determined that increasing the Ti content significantly increased the recrystallization temperature. Toroghinejad and Dini [100] also observed that the recrystallization temperature increased with the increase in Ti content. The deformed ferrite microstructure was insufficient for complete recrystallization at an annealing temperature of 943 K adopted in the steel industry, and a higher recrystallization temperature was required. Mao [35] discovered that nanoscale TiC particles hindered the movement of dislocations and inhibited the generation of recrystallization grains in cold-rolled steel during annealing at temperatures lower than 913 K. Therefore, compared with low-carbon Ti-free steel, Ti-bearing steel requires a higher recrystallization temperature for Ostwald coarsening of TiC particles, thereby promoting the generation of recrystallized grains.

5. Multiple Ti microalloying technology

Precipitation strengthening is an effective and economical method to improve the strength of steel. Meanwhile, precipitation strengthening does not significantly damage the initial properties of steel. Therefore, increasing the amount of precipitation to maximize the strengthening effect is a practical approach to increase the performance of steel. The reasonable addition of various microalloying elements, i.e., multiple microalloying technology, can not only increase the volume of the precipitated phase but also refine the size of precipitated particles [101–104]. Thus, multiple microalloying technology is a powerful approach to enhance the precipitation strengthening effect. Based on Ti microalloying, multiple microalloying technology by adding Ti with Nb, V, Mo, and other elements has been proposed. The stability of carbides and nitrides of V, Nb, and Ti in microalloying elements increases gradually, and the solubility of nitrides and carbides of Ti and V significantly differs. Therefore, the beneficial effects of carbides and nitrides of different microalloying elements can be fully explored by adjusting the contents of microalloying elements and the manufacturing process, which is a key point and a difficult technique in multiple microalloying.

TiC has a small density, ideal chemical ratio, and large precipitation strengthening potential because of nanoscale precipitates at low temperatures. The high thermal stability of TiN, TiO, and other Ti-based precipitations ensures that the microstructures are refined at high temperatures. Therefore, Ti-based multiple microalloying technology has become the most effective method to achieve precipitation strengthening. Combined with TMCP technology, Ti-based multiple microalloying technology can not only realize strong precipitation strengthening capability but also refine the grain size of steel, thereby considerably improving the mechanical properties of steel.

Kashima *et al.* [105–106] analyzed the relationship between the rolling parameters and the microstructure and properties of Ti-microalloyed steel. They determined that reducing the coiling temperature can significantly increase the tensile strength of steel. Yield strength of approximately 700 MPa and tensile strength of approximately 790 MPa with a good hole expansion rate can be obtained after 1173 K finish rolling and 723 K coiling. Kamibayashi *et al.* [107] reported that the addition of 0.12wt% Ti can more effectively refine ferrite grains than the addition of 0.22wt% Nb, which is more conducive to improve the overall performance of the investigated steel. Zhou *et al.* [108] developed high-strength low-carbon weathering steel and container plate steel with Ti contents less than 0.2wt%. High yield strength of 450–700 MPa could be obtained, of which the TiC secondary phase particles with a volume fraction of 27% (relative to the volume of total particles) and an average size smaller than 10 nm contribute approximately 156 MPa strengthening effect.

Based on the characteristics of TSCR technology, Mao *et al.* [109–110] and Gao *et al.* [111] developed a series of high-strength microalloyed steel plates using single Ti microalloying technology. They showed that the addition of approximately 0.2wt% Ti can reduce the average grain size of ferrite, resulting in a strong fine-grain strengthening effect.

The strengthening of dispersion-distributed TiC precipitations exceeded 150 MPa. Yong [112] systematically examined the precipitation sequence, morphology, and orientation relationship of carbides with the sizes of 2–10 nm in Ti-microalloyed steel. Table 1 lists the chemical compositions of hot-rolled Ti-microalloyed high-strength steels.

Table 1. Main chemical compositions of Ti-microalloyed high-strength steels [35] wt%

Steel type	C	Si	Mn	Nb	Ti	Mo	V	Cr
S700MC	≤0.12	≤0.60	≤2.1	≤0.09	≤0.1	—	≤0.20	—
ZJ700W	≤0.07	≤0.60	≤2.0	—	≤0.15	—	—	≤0.6
Kashima	0.03	1.0	1.4	—	0.13	—	—	—
Kestenbach	0.11	0.28	1.54	0.04	0.11	—	—	—
Charlleux	0.07	0.14	1.35	0.086	0.047	—	—	—
Ghosh	0.05	0.14	1.53	—	0.097	0.21	—	—
Domex	≤0.12	≤0.10	≤2.1	≤0.09	≤0.15	—	≤0.20	—
Funakawa	0.047	0.22	1.59	—	0.082	0.20	—	—

The volume fraction, size, shape, and distribution of the secondary phase particles are closely related to the properties of microalloyed steel. The critical issue in maximizing the precipitation strengthening effect is to obtain nanoscale precipitates with large volume fraction, small size, and uniform dispersion. Notably, the V–Ti–N-microalloyed steel series exhibits high grain coarsening temperature, low grain coarsening rate, and low recrystallization temperature. TiN precipitates at high temperatures reduce the N content in austenite, thereby suppressing the precipitation of VN during hot rolling. The precipitation rate of VN during ferrite transformation at low temperatures can be increased; consequently, the strength of steel can be enhanced. Nb–Ti-microalloyed steel also employs the precipitation of TiN in liquid or austenite at high-temperature zones. When the Ti content exceeds 0.011wt%, TiN inhibits the subsequent solidification process and the growth of austenite grains in δ–γ phase transformation.

Charleux *et al.* [14] applied Ti–Nb multiple microalloying and obtained a yield strength of 648 MPa and a tensile strength of 720 MPa in low-carbon steel when coiling at 923 K, in which the precipitation strengthening was 230–239 MPa. Chun *et al.* [113] achieved a tensile yield strength of 990 MPa and a hole expansion rate of 65% in Nb–V–Ti multiple microalloyed steel when coiled at 923 K. Lu and Wang [114] microalloyed a steel using Ti and Nb elements and obtained a yield strength of more than 700 MPa. Carbide precipitation in the ferrite matrix contributed approximately 200 MPa to the total strength. Automobile beam steel with tensile strengths of 700–780 MPa has been developed using Ti–Nb multiple microalloying technology combined with optimized controlled rolling and controlled cooling technologies [115–118].

In Ti–Mo-microalloyed steel, the addition of Mo can increase the solid solubility of Ti in austenite, significantly enhancing the precipitation strengthening effect of TiC and increasing the utilization rate of Ti [119]. Notably, the addition of more than 0.15wt% Mo significantly affects the phase transformation and MC phase precipitation. Mo refines the ferrite grains and coprecipitates with Nb, V, and Ti, increasing the total amount of precipitations and refining the MC phase particles at the same time. For example, Ti–Mo multiple microalloying technology was used to prepare 780 MPa high-strength steel used for automobile parts [87,120].

The addition of V based on Ti–Mo multiple microalloying can further improve the precipitation strengthening effect of steel and achieve ultrahigh strength in microalloyed steel. By combining Ti–Mo–V multiple microalloying technology and the appropriate TMCP, Zhang *et al.* [121–122] developed several ultrahigh-strength steels with yield strengths of 900−1000 MPa. Steel with 0.16wt% C–0.2wt% Ti–0.44wt% Mo–0.41wt% V had a yield strength of 1080 MPa and a tensile strength of 1134 MPa. The precipitation strengthening contribution of (Ti,V,Mo)C particles with sizes less than 10 nm exceeded 400 MPa.

6. Conclusions and perspective

As an important microalloying element, Ti considerably affects the microstructures and properties of microalloyed steel, and its performance is closely related to its form of existence in steel, e.g., Ti-contained inclusions and precipitates. By controlling the precipitation of Ti-containing secondary phases, as well as the number, size, and distribution of these precipitates, during different stages of steel manufacturing processes, grains of steel can be considerably refined and strong strengthening effects can thus be obtained, which significantly improves the mechanical properties of microalloyed steel.

(1) During the smelting process, Ti and O form oxides at high temperatures because of their high affinity and precipitate in molten steel. Consequently, these Ti-containing oxide inclusions with the appropriate size and number can hinder the grain growth of high-temperature austenite, thereby refining the austenite grains. Moreover, these inclusions can act as nucleation sites for the austenite to ferrite phase transformation, thereby effectively promoting the formation of acicular ferrite and improving the strength and toughness of Ti-microalloyed steel.

(2) Coarse TiN particles form in liquid steel with a high ratio of N to Ti, which deteriorates the properties of the final products of microalloyed steel. However, thin slab continu-

ous rolling technology can effectively refine the size of liquid TiN because of its high cooling rate during solidification, thereby improving the properties of steel and increasing the utilization rate of Ti.

(3) TiC precipitates form during the soaking process at high temperatures. These particles can hinder the grain growth of austenite more significantly than other microalloying elements contained in particles. TiN, which also precipitates at high temperatures, has a low coarsening rate because of its high thermal stability and small solid solubility product. Thus, TiN can effectively pin the austenite grain boundaries during the heating and isothermal processes. TiN particles can also be used as heterogeneous nucleation sites for ferrite, thereby promoting the formation of an equiaxed ferrite structure.

(4) Excluding the Ti-contained particles formed at high temperatures, the remaining Ti is mainly in the form of TiC through deformation-induced precipitation in austenite during the hot rolling process and through precipitation in supersaturated ferrite during the cooling and coiling processes. The deformation-induced TiC particles have a strong pinning effect on the grain growth and can refine the grains of austenite, resulting in a fine-grained ferrite after post-hot-rolling phase transformation. The TiC precipitations in supersaturated ferrite have small sizes and contribute a strong precipitation strengthening. The refined grain sizes and dispersed nano-sized TiC particles are the main reasons for the excellent mechanical properties of Ti-microalloyed steel.

(5) As a microalloying element, Ti has a low cost and significant strengthening effect. Thus, Ti has been widely used in the steel industry. Based on Ti microalloying, multiple microalloying technologies with additions of Ti with Nb, V, Mo, and other elements, which can take full advantage of the synergy of various microalloying elements and optimize their precipitation strengthening effect, have been developed.

(6) Because of the high chemical activity of Ti, the processing steps of Ti-microalloyed steel must be precisely controlled to increase the effective Ti content in steel and maximize the strengthening effect of Ti. The future development direction of Ti microalloying technology is to expand its application in other steels by exploiting its unique features in chemical and physical metallurgies coupled with multiple microalloying with other elements.

Acknowledgements

This work was financially support by the National Natural Science Foundation of China (Nos. 52104369 and 52071038), the China Postdoctoral Science Foundation (No. 2021M700374), and the State Key Laboratory for Advanced Metals and Materials (No. 2020Z-02).

Conflict of Interest

The authors declare that they have no known competing financial interests or personal relationships that could have appeared to influence the work reported in this paper.

References

[1] M. Ren, P.T. Lu, X.R. Liu, M.S. Hossain, Y.R. Fang, T. Hanaoka, B. O'Gallachoir, J. Glynn, and H.C. Dai, Decarbonizing China's iron and steel industry from the supply and demand sides for carbon neutrality, *Appl. Energy*, 298(2021), art. No. 117209.

[2] L. Dong, G.Y. Miao, and W.G. Wen, China's carbon neutrality policy: Objectives, impacts and paths, *East Asian Policy*, 13(2021), No. 1, p. 5.

[3] P. Kah, M. Pirinen, R. Suoranta, and J. Martikainen, Welding of ultra high strength steels, *Adv. Mater. Res.*, 849(2013), p. 357.

[4] T.M. Noren, *Columbium as a Micro-alloying Element in Steels and Its Effect on Welding Technology*, Ship Structure Committee, Washington, 1963.

[5] Y. Liu, Y.H. Sun, H.T. Wu, Effects of chromium on the microstructure and hot ductility of Nb-microalloyed steel, *Int. J. Miner. Metall. Mater.*, 28(2021), No. 6, p. 1011.

[6] C.F. Yang and Y.Q. Zhang, Applications of V–N microalloying technology in HSLA steels, *Iron Steel*, 37(2002), No. 11, p. 42.

[7] J.Y. Fu, Development history of Nb-microalloying technology and progress of Nb-microalloyed steel, *Iron Steel*, 40(2005), No. 8, p. 1.

[8] R.D.K. Misra, H. Nathani, J.E. Hartmann, and F. Siciliano, Microstructural evolution in a new 770 MPa hot rolled Nb–Ti microalloyed steel, *Mater. Sci. Eng. A*, 394(2005), No. 1-2, p. 339.

[9] G. Xu, X.L. Gan, G.J. Ma, F. Luo, and H. Zou, The development of Ti-alloyed high strength microalloy steel, *Mater. Des.*, 31(2010), No. 6, p. 2891.

[10] E. López-Chipres, I. Mejía, C. Maldonado, A. Bedolla-Jacuinde, M. El-Wahabi, and J.M. Cabrera, Hot flow behavior of boron microalloyed steels, *Mater. Sci. Eng. A*, 480(2008), No. 1-2, p. 49.

[11] M.G. Akben, T. Chandra, P. Plassiard, and J.J. Jonas, Dynamic precipitation and solute hardening in a titanium microalloyed steel containing three levels of manganese, *Acta Metall.*, 32(1984), No. 4, p. 591.

[12] S.J. Chen, L.J. Li, Z.W. Peng, X.D. Huo, and H.B. Sun, On the correlation among continuous cooling transformations, interphase precipitation and strengthening mechanism in Ti-microalloyed steel, *J. Mater. Res. Technol.*, 10(2021), p. 580.

[13] R. Yoda, I. Tsukatani, T. Inoue, and T. Saito, Effect of chemical composition on recrystallization behavior and *r*-value in Ti-added ultra low carbon sheet steel, *ISIJ Int.*, 34(1994), No. 1, p. 70.

[14] M. Charleux, W.J. Poole, M. Militzer, and A. Deschamps, Precipitation behavior and its effect on strengthening of an HSLA-Nb/Ti steel, *Metall. Mater. Trans. A*, 32(2001), No. 7, p. 1635.

[15] C.F. Meng, Y.D. Wang, Y.H. Wei, B.Q. Shi, T.X. Cui, and Y.T. Wang, Strengthening mechanisms for Ti- and Nb–Ti-micro-alloyed high-strength steels, *J. Iron Steel Res. Int.*, 23(2016), No. 4, p. 350.

[16] Y.T. Chen, A.M. Guo, and P.H. Li, Nitride and carbonitride precipitation behavior in a Nb–Ti microalloyed extra low carbon HSLA steel, *Heat Treat. Met.*, 32(2007), No. 9, p. 51.

[17] E.O. Hall, The lüders deformation of mild steel, *Proc. Phys. Soc. London Sect. B*, 64(1951), No. 12, p. 1085.

[18] N.J. Petch, The cleavage strength of polycrystals, *J. Iron Steel Inst.*, 174(1953), p. 25.

[19] W.B. Morrison, The effect of grain size on the stress–strain relationship in low-carbon steel, *Trans. Am. Soc. Met.*, 59(1966), No. 4, p. 824.

[20] A.T. Davenport, L.C. Brossard, and R.E. Miner, Precipitation in microalloyed high-strength low-alloy steels, *JOM*, 27(1975), No. 6, p. 21.
[21] T. Gladman, D. Dulieu, and I.D. McIvor, Structure–property relationships in high-strength microalloyed steels, [in] *Proc. of Symp. on Microalloying 75*, New York, 1976.
[22] Y. Tanaka, Progress in TMCP technology and expansion of its range of application, [in] *ASME 2005 Pressure Vessels and Piping Conference*, Denver, 2005, p. 515.
[23] Z.H. Wu, W. Zheng, G.Q. Li, H. Matsuura, and F. Tsukihashi, Effect of inclusions' behavior on the microstructure in Al–Ti deoxidized and magnesium-treated steel with different aluminum contents, *Metall. Mater. Trans. B*, 46(2015), No. 3, p. 1226.
[24] B. López and J.M. Rodriguez-Ibabe, Some metallurgical issues concerning austenite conditioning in Nb–Ti and Nb–Mo microalloyed steels processed by near-net-shape casting and direct rolling technologies, *Metall. Mater. Trans. A*, 48(2017), No. 6, p. 2801.
[25] Y.Z. Lou, D.L. Liu, X.P. Mao, and M.Z. Bai, Titanium carbonitrides in Ti-microalloyed steel produced by CSP process, *Iron Steel.*, 45(2010), No. 2, p. 70.
[26] J.M. Rodriguez-Ibabe, Thin slab direct rolling of microalloyed steels, *Mater. Sci. Forum*, 500-501(2005), p. 49.
[27] C.Y. Chen, H.W. Yen, F.H. Kao, W.C. Li, C.Y. Huang, J.R. Yang, and S.H. Wang, Precipitation hardening of high-strength low-alloy steels by nanometer-sized carbides, *Mater. Sci. Eng. A*, 499(2009), No. 1-2, p. 162.
[28] T.P. Wang, F.H. Kao, S.H. Wang, J.R. Yang, C.Y. Huang, and H.R. Chen, Isothermal treatment influence on nanometer-size carbide precipitation of titanium-bearing low carbon steel, *Mater. Lett.*, 65(2011), No. 2, p. 396.
[29] H.W. Yen, C.Y. Huang, and J.R. Yang, Characterization of interphase-precipitated nanometer-sized carbides in a Ti–Mo-bearing steel, *Scripta Mater.*, 61(2009), No. 6, p. 616.
[30] A.J. deArdo, Metallurgical basis for thermomechanical processing of microalloyed steels, *Ironmaking Steelmaking*, 28(2001), No. 2, p. 138.
[31] J.H. Jang, C.H. Lee, Y.U. Heo, and D.W. Suh, Stability of (Ti,M)C (M = Nb, V, Mo and W) carbide in steels using first-principles calculations, *Acta Mater.*, 60(2012), No. 1, p. 208.
[32] C. Leyens and M. Peters, *Titanium and Titanium Alloys. Fundamentals and Applications*, Willey-VCH, Weinheim, 2003.
[33] A.D. McQuillan and M.K. McQuillan, *Titanium*, Butterworths Scientific Publications, London, 1956.
[34] H.H. Read, *Rutley's Elements of Mineralogy*, 25th ed., Thomas Murby & Co., London, 1953.
[35] X.P. Mao, *Titanium Microalloyed Steel*, Metallurgical Industry Press, Beijing, 2016.
[36] E. Orowan, Discussion on internal stresses, [in] *Symposium on International Stresses in Metals and Alloys*, Institute of Metals, London, 1948, p. 451.
[37] X.P. Mao, X.J. Sun, Y.L. Kang, and Z.Y. Lin, Physical metallurgy for the titanium microalloyed strip produced by thin slab casting and rolling process, *Acta Metall. Sin.*, 42(2006), No. 10, p. 1091.
[38] M.L. Wang, G.G. Cheng, S.T. Qiu, P. Zhao, and Y. Gan, Behavior of precipitation containing titanium during solidification, *J. Iron Steel Res. Int.*, 19(2007), No. 5, p. 44.
[39] J.X. Chen, *Manual of Chart and Data in Common Use of Steelmaking*, Metallurgy Industry Press, Beijing, 1984.
[40] J.I. Takamura and S Mizoguchi, Role of oxides in steel performance, [in] *Proceeding of the 6th International Iron and Steel Congress*, Nagoya, 1990, p. 591.
[41] Z.Z. Liu and M. Kuwabara, Recent progress in oxide metallurgy technology and its application, *Steelmaking*, 23(2007), No. 4, p. 1.
[42] K. Yamamoto, T. Hasegawa, and J.I. Takamura, Effect of boron on intra-granular ferrite formation in Ti-oxide bearing steels, *ISIJ Int.*, 36(1996), No. 1, p. 80.
[43] J.H. Shim, Y.W. Cho, S.H. Chung, J.D. Shim, and D.N. Lee, Nucleation of intragranular ferrite at Ti_2O_3 particle in low carbon steel, *Acta Mater.*, 47(1999), No. 9, p. 2751.
[44] L.N. Han, Y.P. Bao, J.H. Liu, and T.Q. Li, Research on nucleation mechanism of IGF of low carbon steel containing titanium, *Wide Heavy Plate*, 14(2008), No. 1, p. 1.
[45] A. Takeuchi and A. Inoue, Classification of bulk metallic glasses by atomic size difference, heat of mixing and period of constituent elements and its application to characterization of the main alloying element, *Mater. Trans.*, 46(2005), No. 12, p. 2817.
[46] K. Inoue, I. Ohnuma, H. Ohtani, K. Ishida, and T. Nishizawa, Solubility product of TiN in austenite, *ISIJ Int.*, 38(1998), No. 9, p. 991.
[47] K. Narita, Physical chemistry of the groups IVa (Ti, Zr), Va (V, Nb, Ta) and the rare earth elements in steel, *Trans. ISIJ*, 15(1975), No. 3, p. 145.
[48] M. Gómez, L. Rancel, P.P. Gómez, J.I. Robla, and S.F. Medina, Simplification of hot rolling schedule in Ti-microalloyed steels with optimised Ti/N ratio, *ISIJ Int.*, 50(2010), No. 6, p. 868.
[49] R. Kuziak, T. Bołd, and Y.W. Cheng, Microstructure control of ferrite–pearlite high strength low alloy steels utilizing microalloying additions, *J. Mater. Process. Technol.*, 53(1995), No. 1-2, p. 255.
[50] S.Y. Lee, Y.J. Oh, and K.W. Yi, Effects of titanium and oxygen content on microstructure in low carbon steels, *Mater. Trans.*, 43(2002), No. 3, p. 518.
[51] L.D. Xing, J.L. Guo, X. Li, Z.F. Zhang, M. Wang, Y.P. Bao, F.Z. Zeng, and B.T. Chen, Control of TiN precipitation behavior in titanium-containing micro-alloyed steel, *Mater. Today Commun.*, 25(2020), art. No. 101292.
[52] T. Liu, M.J. Long, D.F. Chen, H.M. Duan, L.T. Gui, S. Yu, J.S. Cao, H.B. Chen, and H.L. Fan, Effect of coarse TiN inclusions and microstructure on impact toughness fluctuation in Ti micro-alloyed steel, *J. Iron Steel Res. Int.*, 25(2018), No. 10, p. 1043.
[53] J. Fu, J. Zhu, L. Di, F.S. Tong, D.L. Liu, and Y.L. Wang, Study on the precipitation behavior of TiN in the microalloyed steels, *Acta Metall. Sin.*, 36(2000), No. 8, p. 801.
[54] X. Yang, G.G. Cheng, M.L. Wang, Y.L. Li, Y.G. Wang, and P. Zhao, Precipitation and growth of titanium nitride during solidification of clean steel, *J. Univ. Sci. Technol. Beijing*, 10(2003), No. 5, p. 24.
[55] S. Akamatsu, M. Hasebe, T. Senuma, Y. Matsumura, and O. Akisue, Thermodynamic calculation of solute carbon and nitrogen in Nb and Ti added extra-low carbon steels, *ISIJ Int.*, 34(1994), No. 1, p. 9.
[56] X.H. Yang, D. Vanderschueren, J. Dilewijns, C. Standaert, and Y. Houbaert, Solubility products of titanium sulphide and carbosulphide in ultra-low carbon steels, *ISIJ Int.*, 36(1996), No. 10, p. 1286.
[57] J. Copreaux, H. Gaye, J. Henry, and S. Lanteri, *Relation Précipitation–Propriétés Dans Les Aciers Sans Intersticiels Recuits En Continu*, European Commission, Luxembourg, 1997.
[58] H. Yu, X.Y. Xiong, Y.L. Kang, X. Liu, and Y. Fang, Simulation of precipitation behaviors of the precipitates in Ti-IF steel produced by TSCR process, *Heat Treat. Met.*, 31(2006), No. 5, p. 45.
[59] C.N. Jing, Z.C. Wang, F.T. Han, Y.H. Yi, and W.P. Zhang, Study on the precipitates of Ti-IF steel hot-rolled in ferrite region, *Heat Treat. Met.*, 31(2006), No. 1, p. 79.
[60] W.J. Liu, J.J. Jonas, D. Bouchard, and C.W. Bale, Gibbs ener-

gies of formation of TiS and $Ti_4C_2S_2$ in austenite, *ISIJ Int.*, 30(1990), No. 11, p. 985.
[61] N. Yoshinaga, K. Ushioda, S. Akamatsu, and O. Akisue, Precipitation behavior of sulfides in Ti-added ultra low-carbon steels in austenite, *ISIJ Int.*, 34(1994), No. 1, p. 24.
[62] F.Y. Yan and X.G. Zhang, Application of Ti to automobile wheel steel and discussion on alloying technology, *Iron Steel.*, 36(2001), No. 5, p. 47.
[63] M.J. Whelan, On the kinetics of precipitate dissolution, *Met. Sci. J.*, 3(1969), No. 1, p. 95.
[64] K. Relander, *Austenitzerfall Eines 0.18%C–2%Mo–Stahles in Temperaturbereich der Perlitstufe* [Dissertation], Teknillinen Korkeakoulu, Helsinki, 1964.
[65] T.N. Baker, Titanium microalloyed steels, *Ironmaking Steelmaking*, 46(2019), No. 1, p. 1.
[66] R.M. Smith and D.P. Dunne, Structural aspects of alloy carbonitride precipitation in microalloyed steel, *Mater. Forum*, 11(1988), p. 166.
[67] H.W. Yen, P.Y. Chen, C.Y. Huang, and J.R. Yang, Interphase precipitation of nanometer-sized carbides in a titanium–molybdenum-bearing low-carbon steel, *Acta Mater.*, 59(2011), No. 16, p. 6264.
[68] J.H. Jang, Y.U. Heo, C.H. Lee, H.K.D.H. Bhadeshia, and D.W. Suh, Interphase precipitation in Ti–Nb and Ti–Nb–Mo bearing steel, *Mater. Sci. Technol.*, 29(2013), No. 3, p. 309.
[69] W.B. Morrison and J.H. Woodhead, The influence of small niobium additions on mechanical properties of commercial mild steel, *J. Iron Steel Inst.*, 201(1963), p. 43.
[70] H.I. Aaronson, M.R. Plichta, G.W. Franti, and K.C. Russell, Precipitation at interphase boundaries, *Metall. Trans. A*, 9(1978), No. 3, p. 363.
[71] J.M. Gray and R.B.G. Yeo, Columbium carbonitride precipitation in low-alloy steels with particular emphasis on precipitate-row formation, *Trans. Am. Soc. Met.*, 61(1968), p. 255.
[72] J. McCann and K.A. Ridal, High temperature decomposition of austenite in alloy steels, *J. Iron Steel Inst.*, 202(1964), p. 191.
[73] A.T. Davenport and R.W.K. Honeycombe, Precipitation of carbides at γ–α boundaries in alloy steels, *Proc. R. Soc. London Ser. A*, 322(1971), No. 1549, p. 191.
[74] H.W. Yen, C.Y. Chen, T.Y. Wang, C.Y. Huang, and J.R. Yang, Orientation relationship transition of nanometre sized interphase precipitated TiC carbides in Ti bearing steel, *Mater. Sci. Technol.*, 26(2010), No. 4, p. 421.
[75] R. Okamoto, A. Borgenstam, and J. Ågren, Interphase precipitation in niobium-microalloyed steels, *Acta Mater.*, 58(2010), No. 14, p. 4783.
[76] R.W.K. Honeycombe and R.F. Mehl, Transformation from austenite in alloy steels, *Metall. Trans. A*, 7(1976), No. 7, p. 915.
[77] Y.W. Kim, S.G. Hong, Y.H. Huh, and C.S. Lee, Role of rolling temperature in the precipitation hardening characteristics of Ti–Mo microalloyed hot-rolled high strength steel, *Mater. Sci. Eng. A*, 615(2014), p. 255.
[78] G.L. Dunlop, C.J. Carlsson, and G. Frimodig, Precipitation of VC in ferrite and pearlite during direct transformation of a medium carbon microalloyed steel, *Metall. Trans. A*, 9(1978), No. 2, p. 261.
[79] A.D. Batte and R.W.K. Honeycombe, Precipitation of vanadium carbide in ferrite, *J. Iron Steel Inst.*, 211(1973), No. 4, p. 284.
[80] J.A. Todd, P. Li, and S.M. Copley, A new model for precipitation at moving interphase boundaries, *Metall. Trans. A*, 19(1988), No. 9, p. 2133.
[81] P. Li and J.A. Todd, Application of a new model to the interphase precipitation reaction in vanadium steels, *Metall. Trans. A*, 19(1988), No. 9, p. 2139.
[82] J.A. Todd and Y.J. Su, A mass transport theory for interphase precipitation with application to vanadium steels, *Metall. Trans. A*, 20(1989), No. 9, p. 1647.
[83] J. Irvine and T.N. Baker, The influence of rolling variables on the strengthening mechanisms operating in niobium steels, *Mater. Sci. Eng.*, 64(1984), No. 1, p. 123.
[84] X.P. Mao, J.X. Gao, and Y.Z. Chai, Development of thin slab casting and direct rolling process in China, *Iron Steel*, 49(2014), No. 7, p. 49.
[85] S.F. Medina, M. Chapa, P. Valles, A. Quispe, and M.I. Vega, Influence of Ti and N contents on austenite grain control and precipitate size in structural steels, *ISIJ Int.*, 39(1999), No. 9, p. 930.
[86] E.J. Palmiere, C.I. Garcia, and A.J. De Ardo, Compositional and microstructural changes which attend reheating and grain coarsening in steels containing niobium, *Metall. Mater. Trans. A*, 25(1994), No. 2, p. 277.
[87] Y. Funakawa, Mechanical properties of ultra fine particle dispersion strengthened ferritic steel, *Mater. Sci. Forum*, 706-709(2012), p. 2096.
[88] A.J. DeArdo, Niobium in modern steels, *Int. Mater. Rev.*, 48(2003), No. 6, p. 371.
[89] P. Gordon and R.A. Vandermeer, Grain boundary migration, [in] *Recrystallization, Grain Growth and Textures*, American Society for Metals, Metals Park, Ohio, 1966, p. 205.
[90] A.J. De Ardo, J.M. Gray, and L. Meyer, Fundamental metallurgy of niobium in steel, [in] H. Stuart, ed., *Niobium - Proceedings of The International Symposium*, San Francisco, CA, 1984, p. 685.
[91] H.K.D.H. Bhadeshia, *Interpretation of The Microstructure of Steels*, University of Cambridge, Cambridge, 2008.
[92] J.S. Kirkaldy and D. Venugopalan, Prediction of microstructure and hardenability in low alloy steels, [in] A.R. Marder and J.I. Goldstein, eds., *The International Conference on Phase Transformation in Ferrous Alloys*, Philadelphia, 1983, p. 125.
[93] G.F.V. Voort and G.M. Lucas, Microstructural characterization of carburized steels, *Heat Treat. Prog.*, 9(2009), No. 5, p. 37.
[94] R.A. Farrar and P.L. Harrison, Acicular ferrite in carbon–manganese weld metals: An overview, *J. Mater. Sci.*, 22(1987), No. 11, p. 3812.
[95] G. Krauss and S.W. Thompson, Ferritic microstructures in continuously cooled low- and ultralow-carbon steels, *ISIJ Int.*, 35(1995), No. 8, p. 937.
[96] A. Ali and H.K.D.H. Bhadeshia, Nucleation of Widmanstätten ferrite, *Mater. Sci. Technol.*, 6(1990), No. 8, p. 781.
[97] H.K.D.H. Bhadeshia and J.W. Christian, Bainite in steels, *Metall. Trans. A*, 21(1990), No. 3, p. 767.
[98] H.K.D.H. Bhadeshia and D.V. Edmonds, The mechanism of bainite formation in steels, *Acta Metall.*, 28(1980), No. 9, p. 1265.
[99] J.Y. Choi, B.S. Seong, S.C. Baik, and H.C. Lee, Precipitation and recrystallization behavior in extra low carbon steels, *ISIJ Int.*, 42(2002), No. 8, p. 889.
[100] M.R. Toroghinejad and G. Dini, Effect of Ti-microalloy addition on the formability and mechanical properties of a low carbon (ST14) steel, *Int. J. Iron Steel Soc. Iran*, 3(2006), No. 2, p. 1.
[101] D. Wu, F.M. Wang, J. Cheng, and C.R. Li, Effect of Nb and V on the continuous cooling transformation of undercooled austenite in Cr–Mo–V steel for brake discs, *Int. J. Miner. Metall. Mater.*, 25(2018), No. 8, p. 892.
[102] X.L. Wan, K.M. Wu, G. Huang, R. Wei, and L. Cheng, *In situ* observation of austenite grain growth behavior in the simulated coarse-grained heat-affected zone of Ti-microalloyed steels, *Int. J. Miner. Metall. Mater.*, 21(2014), No. 9, p. 878.

[103] Y.S. Yu, B. Hu, M.L. Gao, Z.J. Xie, X.Q. Rong, G. Han, H. Guo, and C.J. Shang, Determining role of heterogeneous microstructure in lowering yield ratio and enhancing impact toughness in high-strength low-alloy steel, *Int. J. Miner. Metall. Mater.*, 28(2021), No. 5, p. 816.

[104] Z.J. Xie, C.J. Shang, X.L. Wang, X.M. Wang, G. Han, and R.D.K. Misra, Recent progress in third-generation low alloy steels developed under M^3 microstructure control, *Int. J. Miner. Metall. Mater.*, 27(2020), No. 1, p. 1.

[105] T. Kashima, S. Hashimoto, and Y. Mukai, 780 N/mm^2 grade hot-rolled high-strength steel sheet for automotive suspension system, *JSAE Rev.*, 24(2003), No. 1, p. 81.

[106] T. Kashima and Y. Mukai, Development of 780 MPa class high strength hot rolled steel sheet with super high flange formability, *R&D Kobe Steel Eng. Rep.*, 52(2002), No. 3, p. 19.

[107] K. Kamibayashi, Y. Tanabe, Y. Takemoto, I. Shimizu, and T. Senuma, Influence of Ti and Nb on the strength–ductility–hole expansion ratio balance of hot-rolled low-carbon high-strength steel sheets, *ISIJ Int.*, 52(2012), No. 1, p. 151.

[108] J. Zhou, Y.L. Kang, X.P. Mao, Z.Y. Lin, L.J. Li, and W. Chen, Effect of Ti on the mechanical properties of high strength weathering steel, *J. Univ. Sci. Technol. Beijing*, 28(2006), No. 10, p. 926.

[109] X.P. Mao, J.X. Gao, L.J. Li, Q.Y. Liu, Z.Y. Lin, and C.F. Xu, Development and research of 550 MPa high strength and high formability plate, *Automob. Technol. Mater.*, 2006, No. 11, p. 1.

[110] X.P. Mao, X.D. Huo, Q.Y. Liu, Y.L. Kang, Z.Y. Lin, H.Z. Zhuang, X.J. Sun, J. Zhou, and J.X. Gao, Research and application of microalloying technology based on thin slab casting and direct rolling process, [in] *International Symposium on Thin Slab Continuous Casting and Rolling*, Guangzhou, 2006.

[111] J.X. Gao, X.P. Mao, Q.L. Chen, and L.J. Li, Microstructure and property of 700MPa Ti microalloyed high strength steel produced by EAF-CSP, *Adv. Mater. Res.*, 287-290(2011), p. 961.

[112] Q.L. Yong, *Secondary Phases in Steels*, Metallurgical Industry Press, Beijing, 2006.

[113] E.J. Chun, H. Do, S. Kim, D.G. Nam, Y.H. Park, and N. Kang, Effect of nanocarbides and interphase hardness deviation on stretch-flangeability in 998 MPa hot-rolled steels, *Mater. Chem. Phys.*, 140(2013), No. 1, p. 307.

[114] J.X. Lu and G.D. Wang, Study on the performance of carbonitride precipitation in Nb–Ti microalloyed steel, *Iron Steel*, 40(2005), No. 9, p. 69.

[115] X.N. Wang, H.S. Di, and L.X. Du, Effects of deformation and cooling rate on nano-scale precipitation in hot-rolled ultra-high strength steel, *Acta Metall. Sin.*, 48(2012), No. 5, p. 621.

[116] X.N. Wang, L.X. Du, and H.S. Di, Study on fatigue property of new type hot-rolled nano precipitation strengthening ultra-high strength automobile strip, *J. Mech. Eng.*, 48(2012), No. 22, p. 27.

[117] X.N. Wang, L.X. Du, and H.S. Di, Austenitic transformation behavior of hot-rolled 590 MPa grade wheel wteel, *J. Iron Steel Res.*, 25(2013), No. 4, p. 33.

[118] X.N. Wang, L.X. Du, H.L. Zhang, and H.S. Di, Industrial trial of 780 MPa grade heavy-duty truck beams steels, *J. Iron Steel Res.*, 23(2011), No. 5, p. 45.

[119] Y. Funakawa and K. Seto, Coarsening behavior of nanometer-sized carbides in hot-rolled high strength sheet steel, *Mater. Sci. Forum*, 539-543(2007), p. 4813.

[120] Y. Huang, W.N. Liu, A.M. Zhao, J.K. Han, Z.G. Wang, and H.X. Yin, Effect of Mo content on the thermal stability of Ti–Mo-bearing ferritic steel, *Int. J. Miner. Metall. Mater.*, 28(2021), No. 3, p. 412.

[121] K. Zhang, Z.D. Li, X.J. Sun, Q.L. Yong, J.W. Yang, Y.M. Li, and P.L. Zhao, Development of Ti–V–Mo complex microalloyed hot-rolled 900-MPa-grade high-strength steel, *Acta Metall. Sin. Engl. Lett.*, 28(2015), No. 5, p. 641.

[122] K. Zhang, Q.L. Yong, X.J. Sun, Z.D. Li, and P.L. Zhao, Effect of coiling temperature on micro-structure and mechanical properties of Ti–V–Mo complex microalloyed ultra-high strength steel, *Acta Metall. Sin.*, 52(2016), No. 5, p. 371.